Ichthyology & Herpetology 110, No. 3, 2022, 449–465

A New Species of *Sphaerodactylus* (Gekkota: Sphaerodactylidae) from the Northwest Limestone Region of Puerto Rico

Alondra M. Díaz-Lameiro[1,2], Catalina I. Villamil[3], Tony Gamble[4,5,6], Brendan J. Pinto[4,7], Alexandra Herrera-Martínez[8], Richard Thomas[9], Justin M. Bernstein[10], James E. Titus-McQuillan[11], Stuart V. Nielsen[12,13], Eliacim Agosto-Torres[1], Alberto R. Puente-Rolón[1], Fernando J. Bird-Picó[1], Taras K. Oleksyk[1,14,15], Juan Carlos Martínez-Cruzado[1], and Juan D. Daza[16]

Advances in both morphological and molecular techniques have uncovered many lineages across the tree of life, and Neotropical vertebrates are no exception. *Sphaerodactylus* geckos (Sphaerodactylidae) are abundant and important components of the Neotropical herpetofauna, but few studies have thoroughly investigated them using a combination of morphology and modern molecular genetic methods. Here, we combine morphological and genetic data to describe a new species of *Sphaerodactylus* from the northwestern karst region of Puerto Rico. The new species is compared to other closely related and sympatric species of *Sphaerodactylus*. Morphological analysis shows that the combination of small body size (median SVL = 21.5 mm), lepidosis, skull morphology, and coloration of the head differentiates the new species from its closest relatives, including the related species, *Sphaerodactylus klauberi*. Comparing sequences of the mitochondrial *16S* rRNA gene showed a genetic distance between *S. klauberi* and the new species of 5.1–5.6%, which is similar to genetic distances among other recognized gecko species. This is the first new species of *Sphaerodactylus* to be described from Puerto Rico in nearly a century, highlighting the continued need to evaluate and chronicle biological diversity even in well-studied regions.

Las filogenias moleculares han elucidado múltiples linajes en el árbol de la vida, incluyendo varios vertebrados neotropicales. Las salamanquitas del género *Sphaerodactylus* (Sphaerodactylidae) son abundantes y forman una parte importante de la herpetofauna neotropical. Este género ha sido investigado recientemente utilizando métodos moleculares modernos. En este artículo se describe una nueva especie del género *Sphaerodactylus*, procedente de la región kárstica del noroeste de Puerto Rico. Los individuos de la nueva especie fueron comparados con especies afines y simpátricas. El análisis morfológico muestra que la combinación entre el tamaño corporal, escamación, morfología del cráneo y coloración cefálica, distinguen a la especie nueva de otras especies cercanas filogenéticamente, incluyendo su especie hermana *Sphaerodactylus klauberi*. Al comparar secuencias del gen mitocondrial *16S* rRNA se observó una distancia genética de 5.1–5.6% entre la especie nueva y *S. klauberi*, dicha distancia es similar a la que existe entre otras especies descritas de salamaquitas. Ha pasado casi un siglo desde que la última especie de *Sphaerodactylus* de Puerto Rico fue descrita, ésto resalta la necesidad de seguir evaluando y catalogando la biodiversidad, inclusive en áreas que han sido investigadas a profundidad.

[1] Department of Biology, University of Puerto Rico at Mayagüez, PO Box 9000, Mayagüez, Puerto Rico 00681-9000; Email: (AMDL) alondra.diaz@upr.edu; (EAT) eliacim.agosto@upr.edu; (ARPR) alberto.puente@upr.edu; (FJBP) fernando.bird@upr.edu; and (JCMC) juancarlos.martinez@upr.edu. Send correspondence to AMDL.

[2] Department of Biological Sciences, Towson University, Towson, Maryland.

[3] Doctor of Chiropractic Program, School of Health and Allied Sciences, Universidad Central del Caribe, PO Box 60327, Bayamón, Puerto Rico 00960-6032; Email: catalina.villamil@uccaribe.edu.

[4] Milwaukee Public Museum, Milwaukee, Wisconsin 53233; Email: (TG) tgamble@geckoevolution.org.

[5] Department of Biological Sciences, Marquette University, Milwaukee, Wisconsin 53201.

[6] Bell Museum of Natural History, University of Minnesota, St. Paul, Minnesota 55113.

[7] Center for Evolutionary Medicine & Public Health, Arizona State University, Tempe, Arizona 85281; Email: brendanjohnpinto@gmail.com.

[8] Texas Research Institute for Environmental Studies, Sam Houston State University, Huntsville, Texas 77341; Email: hm.alexandra@gmail.com.

[9] Biology Department, University of Puerto Rico, PO Box 23360, Río Piedras, Puerto Rico 00931-3360, Puerto Rico; Email: richard.jpr32@gmail.com.

[10] Department of Biological Sciences, Rutgers University–Newark, 360 Dr. Martin Luther King Jr. Blvd., Hill Hall 325, Newark, New Jersey 07102; Email: jmbernst223@gmail.com.

[11] Department of Bioinformatics and Genomics, University of North Carolina at Charlotte, 9201 University City Boulevard, Charlotte, North Carolina 28223; Email: jmcquil2@uncc.edu.

[12] Department of Biological Sciences, Louisiana State University Shreveport, Shreveport, Louisiana; Email: stuart.nielsen@lsus.edu.

[13] Division of Herpetology, Florida Museum of Natural History, 3215 Hull Rd., Gainesville, Florida 32611.

[14] Department of Biological Sciences, Oakland University, 318 Meadow Brook Rd., Rochester, Michigan 48309; Email: oleksyk@oakland.edu.

[15] Biology Department, Uzhhorod National University, Uzhhorod, Ukraine.

[16] Department of Biological Sciences, Sam Houston State University, 2000 Avenue I, Life Sciences Building Room 105, Huntsville, Texas 77341; Email: juand.daza@gmail.com.

Submitted: 30 August 2020. Accepted: 16 January 2022. Associate Editor: B. L. Stuart.

 DOI: 10.1643/h2020123 Published online: 23 August 2022

GEOGRAPHICALLY complex landforms are often associated with elevated levels of biodiversity. Nearly 28% of Puerto Rico's land cover is limestone, marked by steep cliffs, deep valleys, and constant rolling hills, largely divided into two geographically discrete regions (Lugo et al., 2001). The northern limestone area is characterized by a large karst formation known as the karst belt (Monroe, 1976) dominated by moist or wet forest. In contrast, the southern limestone area is more arid and covered by dry forest. Yet both of these rugged terrains are hard to penetrate, develop, and explore, representing some of the least disturbed karst environments in the Caribbean. Because of this natural protection, a diverse and unique flora and fauna can be found in Puerto Rico's limestone regions. The karst belt reptile fauna, for example, is represented by 13 extant families (Lugo et al., 2001) and 19 genera, many of which are represented by multiple species, such as *Anolis* (8 species), *Antillotyphlops* (2 species), *Amphisbaena* (2 species), and *Sphaerodactylus* (6 species), several of which are endemic to the region (Rivero, 1998; Lugo et al., 2001). This combination of limited accessibility and unique habitat suggests Puerto Rico's karst region may still harbor undescribed taxa, particularly among the understudied *Sphaerodactylus* geckos.

Sphaerodactylus geckos are abundant and important components of the Neotropical herpetofauna. Although not as well studied as the Caribbean *Eleutherodactylus* and *Anolis*, their habitat and species diversity is notable. Members of this genus are commonly known as sphaeros, salamanquitas, geckolets, or dwarf geckos; although see Baeckens et al. (2020) who recommends discontinuing use of the latter due to its negative connotation. *Sphaerodactylus* are frequently found in large congregations (López-Ortiz and Lewis, 2002; Steinberg et al., 2007; Allen and Powell, 2014), occupying the forest leaf litter microhabitat (Barbour, 1921; Schwartz, 1973; Henderson and Powell, 2009), and in population densities that are among the highest reported for any terrestrial vertebrate (Rodda et al., 2001). Over 100 species live on the Caribbean Islands and in the coastal parts of Central and South America (Schwartz and Henderson, 1991; Gamble et al., 2008). Species of *Sphaerodactylus* are typically minute or miniaturized (Thomas, 1965; MacLean, 1982, 1985; Thomas et al., 1992; Daza et al., 2008), ranging from a minimum snout-to-vent length (SVL) of 14 mm (Hedges and Thomas, 2001) to a maximum size slightly larger than 40 mm (Griffing et al., 2018). *Sphaerodactylus* are diverse in morphology, with many species presenting sexual dichromatism. Most species diversity is concentrated across the Caribbean insular areas, where they have developed high levels of endemicity (Grant, 1931).

There are six recognized species of *Sphaerodactylus* geckos in Puerto Rico distributed throughout the main island in a variety of environments (Thomas and Schwartz, 1966; Rivero, 1998; Daza et al., 2019). The most widespread species, *Sphaerodactylus grandisquamis*, inhabits all Puerto Rican climate zones (Pregill, 1981). In contrast, *S. roosevelti*, *S. nicholsi*, and *S. townsendi* occupy dry shrublands, deciduous forests, or rocky outcrops near the coast. *Sphaerodactylus gaigeae* and *S. klauberi* inhabit rainforests and seasonally dry tropical forests at different elevations across the island. These six, together with the endemic species found on smaller islands surrounding Puerto Rico (Mona: *S. monensis*, Monito: *S. micropithecus*, Desecheo: *S. levinsi*) and in the Spanish and British Virgin Islands (*S. beattyi*, *S. inigoi*, *S. macrolepis*, and *S. parthenopion*), form the totality of the *Sphaerodactylus* from the Puerto Rico Area (PRA; Thomas, 1999). Daza et al. (2019) found that the PRA *Sphaerodactylus* (*S. micropithecus* was not included) form a monophyletic group with two subsequent dispersals out of the the PRA to Jamaica (represented by *S. argus*) and to southern Hispaniola (*S. ariasae*, *S. armstrongi*, *S. plummeri*, and *S. streptophorus*). Aside from recent work examining the phylogenetic relationships amongst nominal *Sphaerodactylus* of the PRA and their close relatives, some clades remain data deficient, such as the montane forms, *S. klauberi* and *S. gaigeae*.

Recently, two publications examining molecular data of species of *Sphaerodactylus* from Puerto Rico reported the existence of a distinct lineage of *Sphaerodactylus* from low elevations in the northwestern karstic areas of the island (Díaz-Lameiro et al., 2013; Daza et al., 2019). This northwestern lineage was considered either sister to *S. klauberi* (Díaz-Lameiro et al., 2013: fig. 3; Daza et al., 2019: fig. 4A) or nested within *S. klauberi* (Daza et al., 2019: fig. 5]), depending on the dataset employed. Díaz-Lameiro et al. (2013) found, using mitochondrial data (mtDNA; *12S* + *16S* genes), animals collected from this region consistently formed a clade to the exclusion of other samples of *S. klauberi* (labeled "*Sphaerodactylus* spp." [sic]). Further, these samples were both genetically (≥5.6% divergence at mtDNA, *12S* + *16S*) and morphologically distinct from other described species. Daza et al. (2019: fig. 4A) found, also using mtDNA (*ND2* + *16S* genes), that animals from this region (labeled as "*S. klauberi* [Northwest]") formed a well-supported clade sister to *S. klauberi* from eastern and central highlands. Incorporating nuclear data with mtDNA in a multi-locus species tree showed that northwestern populations formed a clade sister to eastern *S. klauberi* to the exclusion of *S. klauberi* from the central highlands (Daza et al., 2019: fig. 5). Thus, previous molecular phylogenetic work in *Sphaerodactylus* geckos identified a putative species-level lineage from the northwestern karst region of Puerto Rico.

As stated previously, Díaz-Lameiro et al. (2013) identified animals from this northwestern karst region as morphologically distinct from other described species of *Sphaerodactylus*. Indeed, previous morphological observations also described differences among populations of *S. klauberi*. Thomas and Schwartz (1966) reported variation in size, number of internasal scales, and the size of dorsal scales in four geographical samples or clusters within *S. klauberi*. One of the clusters (Cluster I) identified by Thomas and Schwartz (1966) corresponds to the low elevation lineage and was diagnosed using specimens from the northeastern karst region. The authors reported that Cluster 1 differed from the other specimens of *S. klauberi* by their small to moderate size, a variable number of internasal scales (1–6), a low number of dorsal and mid-ventral scale counts, and by displaying variation in the keeling of the ventral scales (Thomas and Schwartz, 1966). Thus, both genetic and morphological data from previous work suggest there are high levels of variation within *S. klauberi* as currently recognized, and taxonomic revision of this group may be warranted.

Using an integrative taxonomic framework, combining morphological and molecular data, we formally describe the lowland northwestern population as a new species, previously referred to as the *S. klauberi* Cluster I (Thomas and

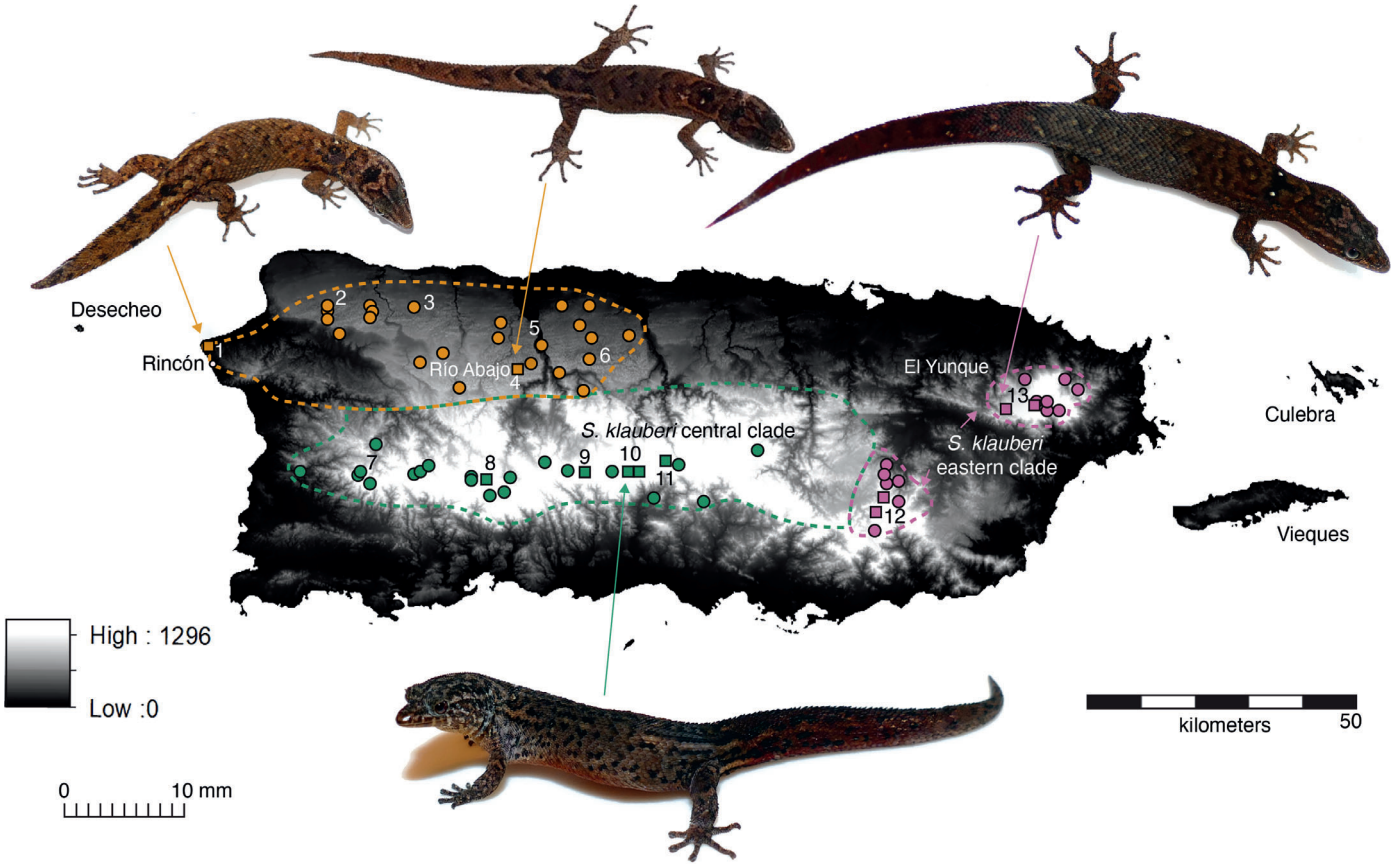

Fig. 1. Proposed distribution of *Sphaerodactylus verdeluzicola*, new species. Orange symbols represent the proposed distribution of the new species; green and pink symbols denote distribution of *S. klauberi*. Circles indicate records from museum databases (*Sphaerodactylus klauberi* in GBIF Secretariat, 2020). Scale bar in mm applies to all pictures of geckos. Museum specimens were examined to confirm if they match the description of the new species. Squares indicate visited localities. 1) Rincón, 2) Isabela, 3) Camuy, 4) Bosque Estatal de Río Abajo, 5) Arecibo, 6) Florida, 7) Maricao, 8) Adjuntas, 9) Toro Negro, 10) Divisoria, 11) Orocovis-Villalba, 12) Bosque Estatal de Carite, 13) El Toro trail.

Schwartz, 1966), *Sphaerodactylus* spp. (Díaz-Lameiro et al., 2013), and *S. klauberi* Northwest clade (Daza et al., 2019). The new species is genetically and morphologically distinct from *S. klauberi* found in high elevations (El Yunque Forest, the Sierra de Cayey, and the Cordillera Central), differing in size, scale and skull morphology, and coloration. The new species is geographically restricted to the northwest karst forest of the main island of Puerto Rico (Fig. 1) and prefers the Subtropical Moist Forest Ecological Life Zone (Ewel and Whitmore, 1973).

MATERIALS AND METHODS

Sampling.—We collected 41 specimens of *Sphaerodactylus* by hand, in leaf litter at two localities along their distributional range (Fig. 1): Bosque Estatal de Río Abajo and Rincón. Specimens were fixed in formaldehyde (following Pisani, 1973). Tissue samples (tail clips) were stored using RNAlater™ Stabilization Solution (ThermoFisher Scientific) during all field seasons. Euthanasia and preservation protocols followed Gamble (2014) and were performed following IACUC protocols.

Morphometric data.—Snout-to-vent length was gathered from all specimens using a Mitutoyo 500-196-30 Digimatic 0-6″/150 mm digital caliper. Live individuals were weighed on site using a KeeKit pocket digital scale. Differences in size and sexual size dimorphism were explored with box plots and Wilcoxon rank sum tests, using the package ggplot2 v3.2.1 (Wickham, 2016) and the R function wilcox.test, respectively, in R v3.6.2 (R Core Team, 2019). Observations of external morphology and scale counts were done on a Leica MS6 dissecting microscope (Leica Microsystems, Wetzlar, Germany). The presence of escutcheon scales was used to distinguish males from females (Grant, 1931).

Microscopy.—Scale microstructure can be an informative characteristic in identification of species of *Sphaerodactylus* (King, 1962; Daza et al., 2019). We used Scanning Electron Microscopy (SEM) to examine the ventral scales of three specimens, two from the new species (Rincón and Bosque Estatal de Río Abajo) and one *S. klauberi* from El Yunque. We also confirmed these characters using a high resolution Keyence Digital Microscope VHX-7000 series. Photographs of the holotype and paratypes were taken using the 3D stitching function on the Keyence VHX-7000. For electron micrographs, samples were adhered to the SEM stub using carbon tape and sputter coated with gold for 60 sec (~200 A) using a Cressington 108. The sputtered samples were imaged under high vacuum at 3–5 kV with a working distance of 5 mm on a Hitachi SU3500 scanning electron microscope using a secondary electron detector. Further image analysis was performed using Fiji software (Schindelin et al., 2012).

Coloration.—Coloration and pattern were initially assessed on high resolution photographs of live specimens ($n = 10$) taken with a Nikon D5300 using the macro setting. These descriptions were verified and expanded on the same specimens after preservation using a 40X magnifying glass and compared to species descriptions (Grant, 1931, 1932a; Thomas and Schwartz, 1966; Daza et al., 2019), available holotype and paratypes images from the Museum of Comparative Zoology at Harvard University (*S. klauberi*, *S. macrolepis guarionex* and *S. macrolepis ateles*, *S. nicholsi*) and the University of Michigan Museum of Zoology (*S. gaigeae*), and additional specimens of *S. klauberi*.

Osteological data.—We collected osteological data using X-rays and high-resolution computed tomography. Digital X-rays were obtained from 21 individuals using a KevexTM PXS10-16W X-ray source and Varian amorphous silicon digital X-ray detector PaxScanH 4030R at the Smithsonian National Museum of Natural History. X-rayed specimens include five of the new species (Florida: USNM 326953, 326954; Bosque Estatal de Río Abajo: JDD 054; Rincón: MPM-RA34016, TG 2643), and 16 from *S. klauberi* (El Yunque: USNM 120719, 326949, 326950, 326952, 326953, 326962; Punta Guilarte: JDD 00401, USNM 326955, 326958, 326959; Jayuya: JDD 00025; Maricao: USNM 292265, 292266, 326956, 326957; Toro Negro: TG 2762). Six specimens were scanned at the University of Texas–High-Resolution X-Ray CT Facility (UTCT), four of the new species, a male and a female from each site, and two from *S. klauberi*. Full body specimens were scanned using an NSI Helical scanner with a Fein Focus High Power source set up at 100 kV, 0.24 mA, and a Perkin Elmer flat-panel detector. Close-ups of the heads were scanned in a Zeiss Xradia 620 Versa with a flat panel objective, 70 kV, 8 W. 3D visualization and models were built using AvizoLite 2019.2 (Thermo Fisher Scientific). Scans will be deposited in Morphosource.org, as part of the National Science Foundation (NSF) Outwardly Mobilizing the UTCT Vertebrate Archive for Research and Training project.

Comparisons.—Morphological comparisons in this paper are based on material from the type locality of *S. klauberi* (El Yunque), sympatric species (*S. nicholsi*, *S. grandisquamis ateles* Thomas and Schwartz 1966, and *S. grandisquamis guarionex* Thomas and Schwartz 1966), and closely related species from Puerto Rico (*S. gaigeae*, *S. roosevelti*, and *S. townsendi*). A total of 54 specimens of *S. klauberi* and 43 new species individuals were examined.

Phylogenetic analysis.—New mitochondrial *16S* rRNA gene sequences were generated from specimens of *S. klauberi* collected near the type locality of El Yunque (TG 2758–2760; Table 1) via Sanger sequencing using published protocols (Gamble et al., 2008). Sequences of *S. klauberi* from individuals collected near the type locality have not been included in any prior phylogenetic analyses and are necessary to distinguish the new species from *S. klauberi sensu stricto*. These sequences were added to previously published *16S* rRNA data from additional species/populations of *Sphaerodactylus* (Díaz-Lameiro et al., 2013; Daza et al., 2019; Pinto et al., 2019; Table 1) and aligned using MUSCLE (Edgar, 2004) implemented in Geneious Prime 2019.2.3 (https://www.geneious.com; Kearse et al., 2012). Due to different primer pairs being used across studies, we trimmed our final alignment to a final length of 374 bp of *16S*. This allows for more concordant genetic data across taxa, limiting long-branch attraction and missing data for a more stable phylogenetic inference. We used these data as input for phylogenetic inference using maximum likelihood and Bayesian methods. The maximum likelihood phylogeny was constructed using IQ-TREE v1.6.10 implementing the best-fit model of sequence evolution (K3Pu+F+G4) chosen according to BIC with 1000 ultrafast bootstrap (UFBoot) replicates on the CIPRES cluster (Miller et al., 2010; Nguyen et al., 2015; Kalyaanamoorthy et al., 2017; Hoang et al., 2018). Bayesian analysis was carried out using BEAST 2.6.2 (Bouckaert et al., 2019) with a Coalescent Constant Population model and a strict clock with a rate set to 1.0 and GTR + G model (Tavaré, 1986). We ran two MCMC chains of 10 million generations each, sampling every 10,000 generations. Output files were checked for convergence using Tracer (Rambaut et al., 2018), and both runs, minus 30% burn-in, were combined to estimate topology. We calculated the net between-group p-distances and standard error, with 100 bootstrap replicates, using MEGA7 v0.26 (Nei and Li, 1979; Kumar et al., 2016).

Population survey and habitat description.—We estimated population densities at the type locality in an effort to better understand the ecology of this new species. On 7–10 June 2019, 36 plots were cleared of plant debris by two surveyors. Plots were chosen based on suitability of habitat for *Sphaerodactylus* and measured with a field measuring tape. Plots were delimited based on convenience, with edges reaching geographical or vegetation boundaries (trails, clifts, overgrown understory). All debris was slowly removed with both researchers starting at opposite corners of the plot and moving towards the middle, counting/capturing all the *Sphaerodactylus* encountered. Once this procedure was done, the leaf litter was placed back into the plot. A total area of 195.81 m^2 was surveyed in three sites, east of Domes beach (14 plots), north of Domes beach (13 plots), and Punta Gorda (12 plots), all within the municipality of Rincón. Twenty-four plots were surveyed between 0730–1130 h (east Domes = 13, north Domes = 4, Punta Gorda = 7), 15 between the hours of 1230–1600 h (east Domes = 4, north Domes = 8, Punta Gorda = 3). Before clearing each plot, leaf litter composition within and 1 m around the plots was noted. Relative humidity and temperature of the leaf litter and air (1 m above the floor) were measured with a Kestrel 3000 weather meter. Soil temperature, relative humidity, and sun exposure of the plot were measured with a soil tester. Elevation and plot coordinates were obtained from a Garmin GPSMAP Handheld GPS System. Sites ranged in elevation from 5–47 m.a.s.l. (east Domes 12–47 m, north Domes 5–31 m, Punta Gorda 7–22 m). Measured environmental factors such as humidity and temperature were independently analyzed with a Single Factor ANOVA test on MiniTab 19.2. This analysis was done to determine if each factor significantly differed between occupied and empty plots.

Sphaerodactylus verdeluzicola, new species

urn:lsid:zoobank.org:act:7203C0C8-379B-412C-9F32-0707DCE5CC97

Figures 1, 2, 3; Tables 1–3

English Common Name: Puerto Rican Karst Gecko
Spanish Common Name: Salamanquita de Monte y Mar

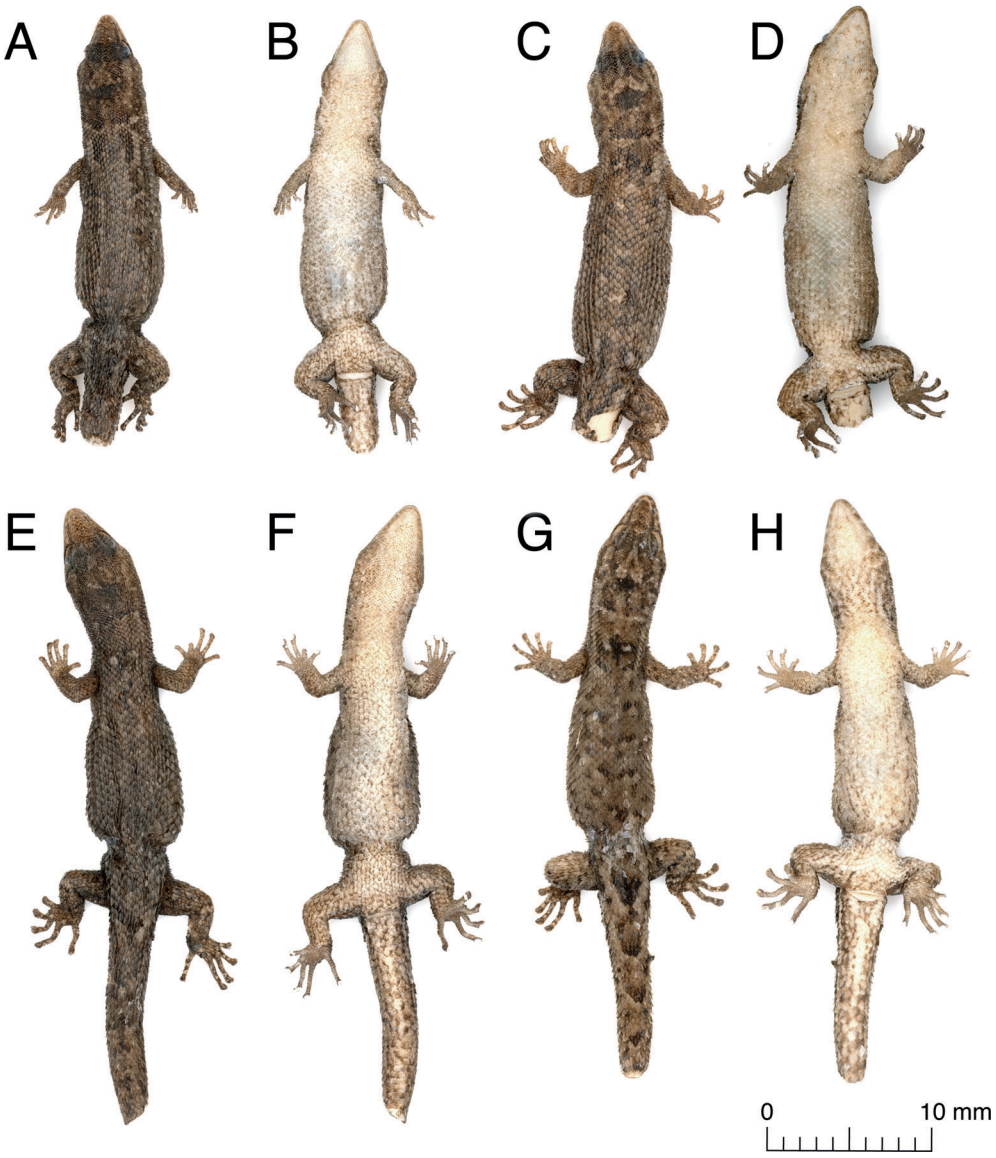

Fig. 2. Dorsal and ventral view of *Sphaerodactylus verdeluzicola* from two localities. Rincón: (A–B) MPM-RA34017, female; (C–D) MPM-RA34016, male, holotype; (E–F) MPM-RA34018, female. Bosque Estatal de Río Abajo: (G–H) MPM-RA34019, male.

Sphaerodactylus klauberi Cluster I Thomas and Schwartz, 1966.
Sphaerodactylus klauberi Thomas and Schwartz, 1975.
Sphaerodactylus klauberi Schwartz and Henderson, 1991.
Sphaerodactylus klauberi Rivero, 1998.
Sphaerodactylus klauberi Rivero, 2006.
Sphaerodactylus spp. Díaz-Lameiro et al., 2013.
Sphaerodactylus klauberi Northwest clade Daza et al., 2019.

Holotype.—MPM-RA34016 (Fig. 2C–D), adult male, Puerto Rico, Rincón, Playa Domes, near the former Boiling Nuclear Superheater Reactor Facility, now Museo Tecnológico Dr. Modesto Iriarte, on the foothills of the mountain behind Road 4413 (18.363880°, –67.267913°) in Barrio Puntas, elevation of 9.4 m.a.s.l., 30 June 2016.

GenBank identifier for holotype* 16S *sequence.—MN414704.

Paratypes.—MPM-RA34017, female (Fig. 2A–B), from the same locality along with the holotype; MPM-RA34018, female (Fig. 2E–F), MPM-RA34019, male (Fig. 2G–H), Bosque Estatal de Río Abajo, 18.333102°, –66.716945°, 2015.

Diagnosis.—*Sphaerodactylus verdeluzicola* was formerly considered a small morphological variant within *S. klauberi* (Cluster I in Thomas and Schwartz [1966]). This species is genetically divergent (Fig. 4) from the high elevation populations restricted here to *S. klauberi sensu stricto* along its distributional range (Fig. 1; Díaz-Lameiro et al., 2013; Daza et al., 2019). *Sphaerodactylus verdeluzicola* can be distinguished from all congeners by the following characters: (1) size (median SVL = 21.50 mm), (2) smooth to partially keeled pectoral scales that are round to rhomboid in shape and either juxtaposed or slightly overlapping, (3) a distinctive club-shaped light cephalic figure, (4) a dark pentagonal parietal patch, (5) a short, steeply inclined nasal process in the premaxilla, (6) a large clavicular fenestra, and (7) a clavicular foramen near the anterior edge.

Externally, *S. verdeluzicola* can be easily differentiated from congeners from Puerto Rico, especially the four species with potentially overlapping ranges: *Sphaerodactylus klauberi* Grant 1931, *Sphaerodactylus nicholsi* Grant 1931, *Sphaerodactylus grandisquamis guarionex* Thomas and Schwartz 1966, and *Sphaerodactylus grandisquamis ateles* Thomas and Schwartz 1966. In size, it is significantly smaller than high elevation *S.*

Fig. 3. Live coloration of *Sphaerodactylus verdeluzicola*. Above, a male specimen from Bosque Estatal de Río Abajo. Below, a female specimen from Rincón.

klauberi (median SVL = 21.50 mm versus 30.83 mm in *S. klauberi*, W = 910, $P = 4.133e^{-10}$; Fig. 5), *S. grandisquamis*, and *S. roosevelti*, although its proportions are similar to other low elevation *Sphaerodactylus* such as *S. gaigeae*, *S. nicholsi*, and *S. townsendi*.

Sphaerodactylus verdeluzicola can be differentiated from *S. roosevelti* and *S. grandisquamis* in the lack of sexual dimorphism and smaller size (Daza et al., 2019). *Sphaerodactylus verdeluzicola* differs from *S. g. guarionex* Thomas and Schwartz 1966 in that *S. verdeluzicola* displays a less marked, lighter, and more diffuse scapular patch. *Sphaerodactylus verdeluzicola* is also smaller in size than *S. g. guarionex* (SVL > 30 mm). Additionally, the pectoral scales are faintly keeled or smooth in *S. verdeluzicola* (Fig. 6) and keeled in *S. g. guarionex*, and the nuchal patch or patches are never continuous with the scapular patch in *S. verdeluzicola*. Unlike *S. g. guarionex*, *S. verdeluzicola* does not display a series of longitudinal dark lines on the dorsum. *Sphaerodactylus verdeluzicola* differs from *S. g. ateles* in that it is smaller than *S. g. ateles* (SVL > 30 mm) and lacks keeled gular scales. The distinctive head and scapular pattern of *S. verdeluzicola* is consistently present in both males and females (Figs. 2, 3), while *S. g. ateles* are sexually dimorphic. The ocelli on the scapular patch of *S. verdeluzicola* are clearly differentiated from the ground color and surrounded by dark lines laterally. The throat of *S. verdeluzicola* lacks the yellow-orange throat coloration of male *S. g. ateles* and the distinctive longitudinal lines on the dorsum of the body of female *S. g. ateles*.

Sphaerodactylus verdeluzicola is similar in appearance and proportions to species from low elevations that have a lighter brown or cream colored dorsum with scattered dark scales, namely *S. nicholsi*, *S. townsendi*, and *S. gaigeae*, the first of these being sympatric with *S. verdeluzicola*. *Sphaerodactylus verdeluzicola* differs from *S. nicholsi* in that *S. verdeluzicola* displays a light, club-shaped cephalic figure (Figs. 2, 3). In addition, *S. nicholsi* has a well-defined crescent-shaped dark mark on the parietal region (Thomas and Schwartz, 1966; Schwartz and Henderson, 1991; Rivero, 1998), while *S. verdeluzicola* displays a solid triangle or pentagon. Color pattern characters also differentiate *S. verdeluzicola* from *S. townsendi*, which has a fragmented pattern of dark patches on the head, and from *S. gaigeae*, which has a ribbon-shaped mark on it (Figs. 2, 3). *Sphaerodactylus verdeluzicola* has a more marked, darker scapular patch with fewer dark blotches on the dorsum compared to *S. gaigeae* (white patches surrounded by dark blotches in the back in *S. gaigeae*; Thomas and Schwartz, 1966; Schwartz and Henderson, 1991; Rivero, 1998), as well as more defined light transverse and dorsolat-

Table 1. List of species of *Sphaerodactylus*, sample IDs, localities, and GenBank IDs for *16S* rRNA gene sequences used in the phylogenetic analysis.

Species	Voucher	Locality	Accession code
S. gaigeae	RT14812	10 mi S on PR184, Puerto Rico	MN414692
	RT14813	11 mi S on PR184, Puerto Rico	MN414693
	RT14851	Mt Pirata, Vieques, Puerto Rico	MN414694
	TG708	North of Maunabo, Puerto Rico	MN414695
S. grandisquamis grandisquamis	RT14660	Piñones, Puerto Rico	MN414639
S. grandisquamis spanius	TG1512	Near Juana Díaz, Puerto Rico	MN414754
S. inigoi	RT14736	Flamenco Beach, Culebra, Puerto Rico	MN414651
	RT14739	Flamenco Beach, Culebra, Puerto Rico	MN414652
	TG2147	Curva de Sixto, Vieques, Puerto Rico	MN414778
S. klauberi	RT14811	near Carite, Puerto Rico	MN414707
	SK-O-2	Orocovis, Puerto Rico	KC840517
	SK-O-4	Orocovis, Puerto Rico	KC840519
	SK-O-8	Orocovis, Puerto Rico	KC840523
	TG694	143/139 junction, Toro Negro, Puerto Rico	MN414708
	TG2013	Divisoria, Puerto Rico	MN414696
	TG2758	El Yunque National Forest - El Toro trail, Puerto Rico	MT452411
	TG2759	El Yunque National Forest - El Toro trail, Puerto Rico	MT452412
	TG2760	El Yunque National Forest - El Toro trail, Puerto Rico	MT452413
	TG2761	Orocovis-Villalba Border - Rd.143 due E, Puerto Rico	MN414697
	TG2762	Orocovis-Villalba Border - Rd.143 due E, Puerto Rico	MN414698
	TG2763	Orocovis-Villalba Border - Rd.143 due E, Puerto Rico	MN414699
	TG3229	Cayey - Bosque Estatal De Carite, Puerto Rico	MN414700
	TG3230	Cayey - Bosque Estatal De Carite, Puerto Rico	MN414701
	TG3231	Cayey - Bosque Estatal De Carite, Puerto Rico	MN414702
	TG3232	Cayey - Bosque Estatal De Carite, Puerto Rico	MN414703
S. levinsi	SL-D-2	Desecheo Island	KC840548
	SL-D-20	Desecheo Island	KC840530
S. macrolepis	STT005	St. Thomas, U.S. Virgin Islands	MN414743
	TG676	Good Hope, St. Croix, U.S. Virgin Islands	MN414749
	TG1936	Zoní Beach, Culebra, Puerto Rico	MN414755
S. monensis	SM-MO-1	Mona Island	KC840571
	SM-MO-2	Mona Island	KC840572
	SM-MO-3	Mona Island	KC840573
	SM-MO-10	Mona Island	KC840579
	SM-MO-17	Mona Island	KC840586
	SM-MO-20	Mona Island	KC840589
S. nicholsi	RT14635	Playa Los Pinos, Camuy, Puerto Rico	MN414714
	RT14637	Playa Los Pinos, Camuy, Puerto Rico	MN414715
	RT14652	Balneario Boquerón, Cabo Rojo, Puerto Rico	MN414716
	RT14657	Balneario Boquerón, Cabo Rojo, Puerto Rico	MN414717
	RT14705	4.4km N/NE Manatí, Puerto Rico	MN414718
	SN-CR-1	Cabo Rojo, Puerto Rico	KC840590
	SN-CR-3	Cabo Rojo, Puerto Rico	KC840591
	SN-CR-4	Cabo Rojo, Puerto Rico	KC840592
	SN-CR-7	Cabo Rojo, Puerto Rico	KC840595
	SN-G-1	Guánica, Puerto Rico	KC840597
	SN-G-3	Guánica, Puerto Rico	KC840599
	SN-G-5	Guánica, Puerto Rico	KC840601
	SN-P-1	Ponce, Puerto Rico	KC840603
	TG2002	Barceloneta, Puerto Rico	MN414764
	TG2030	Park Office, Guánica State Forest, Puerto Rico	MN414766
	TG2096	Balneario Boquerón, Cabo Rojo, Puerto Rico	MK336993
S. parvus	SBH267283	Anguilla	MN414723
	SBH267284	Anguilla	MN414724
S. townsendi	TG210	Salinas, Puerto Rico	MK336984
	TG1505	near Juana Díaz, Puerto Rico	MN414737
	TG2019	Caja de Muertos, Puerto Rico	MN414738
	TG2028	Caja de Muertos, Puerto Rico	MK336987
S. verdeluzicola	SPP-R-2	Rincón, Puerto Rico	KC840560
	SPP-R-10	Rincón, Puerto Rico	KC840568
	SPP-R-11	Rincón, Puerto Rico	KC840569

Table 1. Continued.

Species	Voucher	Locality	Accession code
	SPP-R-12	Rincón, Puerto Rico	KC840570
	TG875	Río Abajo, Puerto Rico	MK337002
	MPM-RA34016	Rincón, Playa Domes, Museo de la Ciencia, Puerto Rico	MN414704

eral lines compared to *S. gaigeae*, which has more chevron-like tail markings.

Another species that occurs geographically closer to *S. verdeluzicola*, although restricted to Desecheo Island, is *S. levinsi*. *Sphaerodactylus verdeluzicola* differs from this species in not having a well-defined dot in the parietal region and the scapular patch less defined, which in *S. levinsi* entirely encloses two ocelli.

Sphaerodactylus verdeluzicola is typically lighter in coloration than *S. klauberi*. In addition, it can be distinguished from *S. klauberi* by a characteristic light-colored cephalic figure resembling a club-shaped marking and a dark brown, pentagonal, parietal patch (Figs. 2, 3). *Sphaerodactylus klauberi* from El Yunque also have rhomboid pectoral scales, but they are more elongated and have keels that are more defined (raised) than in the Río Abajo populations of *S. verdeluzicola* (Fig. 6). Since the number of pectoral scales between the armpits is similar in all the specimens (18–19), scale morphological differences may result from allometric changes. *Sphaerodactylus verdeluzicola* and *S. klauberi* can also differ in the shape of the snout and the clavicular fenestra. In *S. verdeluzicola* (Fig. 7A–C), the lateral view of the snout is proportionally shorter and more steeply inclined than in *S. klauberi* (Fig. 7D–F). The differences in snout shape are mainly due to the ascending nasal process, which in *S. verdeluzicola* expands halfway along its length and tapers gradually to end in a rounded tip (Fig. 7A). In *S. klauberi*, this process tapers gradually (without the expansion) along its entire length, ending in a point (Fig. 7D). The clavicular fenestra in *S. klauberi* and *S. verdeluzicola* is entirely enclosed by bone, but in *S. verdeluzicola* the clavicular fenestra is proportionally larger, resulting in a very thin anterior margin (Fig. 8). The two species also display differences in the position of the clavicular foramen, with *S. verdeluzicola* displaying a foramen near the anterior edge (Fig. 8H) and *S. klauberi* in the middle of the clavicle (Fig. 8G).

Description of holotype.—Body short and stocky; 23.3 mm SVL, postpygal section of the tail absent (clipped for tissue sampling). Head length 7.5 mm (32% SVL), head width 4.1 mm (54.6% head length); anterorbital region triangular with a short and tapering snout, ending on a blunt tip. Scales on

Table 2. Measurements and lamella and scale counts for the holotype and paratypes of *Sphaerodactylus verdeluzicola*.

Variable				
Individual	MPM-RA34016	MPM-RA34017	MPM-RA34018	MPM-RA34019
Specimen designation	Holotype	Paratype	Paratype	Paratype
Locality	Rincón	Rincón	Río Abajo	Río Abajo
Sex	Male	Female	Female	Male
Internasals	3	3	3	3
Loreals	4	4	3	4
Supralabials	3	3	3	3
Infralabials	3	3	3	3
Scales around midbody	46	46	43	41
Lamellae under manual finger 1	3	3	3	3
Lamellae under manual finger 2	5	5	5	6
Lamellae under manual finger 3	7	7	7	7
Lamellae under manual finger 4	8	7	8	8
Lamellae under manual finger 5	3	4	4	4
Lamellae under pedal finger 1	4	4	4	4
Lamellae under pedal finger 2	5	5	5	6
Lamellae under pedal finger 3	9	8	9	9
Lamellae under pedal finger 4	9	9	10	11
Lamellae under pedal finger 5	9	9	10	10
Ventrals between throat (transverse line between anterior border of forelimbs) to posterior border of cloaca	40	38	37	43
Ventrals between axilla and groin	30	26	26	28
Ventrals in transverse line at midbody	19	19	19	19
Postmentals	3	3	4	3
Snout–vent length	23.3	21.8	25.4	24.1
Axilla–groin distance	10.8	8.7	10.8	10.9
Head length (from tip of the snout to transverse pale line in neck)	7.5	6.6	7.4	7.7
Head width	4.1	3.7	4.2	4.2
Scutcheon scales number	66	N/A	N/A	67

Table 3. Net genetic p-distances between groups of closely related Puerto Rican species of *Sphaerodactylus* for a fragment of the mitochondrial *16S* rRNA gene. Standard error estimates, calculated using 100 bootstrap replicates, are shown above the diagonal. All values are calculated as percentages.

	S. gaigeae	*S. klauberi* Central	*S. klauberi* East	*S. levinsi*	*S. monensis*	*S. nicholsi*	*S. townsendi*	*S. verdeluzicola*
S. gaigeae		0.90	1.00	1.10	1.00	0.80	0.90	1.10
S. klauberi Central	4.10		0.70	1.30	1.30	1.20	1.20	1.30
S. klauberi East	6.00	3.10		1.30	1.20	1.10	1.20	1.30
S. levinsi	4.60	6.30	7.50		0.90	1.00	1.00	1.40
S. monensis	3.80	5.80	6.70	3.30		0.70	0.80	1.30
S. nicholsi	2.80	5.10	6.20	3.50	2.10		0.70	1.10
S. townsendi	3.20	5.20	6.40	3.60	2.40	2.00		1.20
S. verdeluzicola	5.00	5.10	5.60	7.00	5.50	4.70	5.20	

snout tend to have a honeycomb pattern towards the midline with low keels, and transition to more elongated scales (but still hexagonal) in the interocular region; scales transition rapidly to about twice as long and wide in the nape region, and keels become more evident. Scales in the neck area are twice as large as the ones in the nape region, there is an irregular patch of scales in the dorsum of the neck (right side) and could be an area that was regenerated as this is not visible in any other specimens. 3 internasals, 4 loreals, 3 supralabials, and 3 infralabials. Pupil rounded, ear opening evident, red iris. Rostral wide with a median cleft and dorsal fissure. Mental scale large forming the entire chin region, 3 postmental scales, first infralabials are slightly wedge shaped, postmental scales are 2 to 3 times larger than the scales in the gular region, postmentals tend to be more juxtaposed, while the ones in the gular region more imbricated. Trunk scales in the dorsum and vent are similar in size, the scales on the dorsum keeled and scales on the vent smooth. The specimen is more pigmented on the dorsum than on the vent, pigmentation in the vent limited to some dark freckles on some scales, and a few light brown scattered scales. The snout is light brown with a well-defined canthal line, supraocular region dark, and a light club-shaped frontal area, followed by a dark pentagonal patch in the parietal region. A less defined dark patch in the nape and neck. No scapular patch with ocelli. Coloration on the dorsum is darker. Approximately 46 scales around the mid-body, and 66 rhomboid, light-colored scutcheon scales (being pigmented only on the edge, forming a dark frame for each scale). Limbs short and stocky, toes free of any webbing, and bearing an apical toe pad. Relative length of digits of manus: I<II<IV<V<III, and of pes: I<II<III<V<IV; digit V of pes in opposition to I–IV.

Description.—*Sphaerodactylus verdeluzicola* is small (median SVL = 21.50 mm) and does not exhibit sexual size dimorphism (Wilcoxon test, $n = 24$, $P = 0.34$; males $\bar{x} =$ 22.30 mm, females $\bar{x} = 21.70$ mm). Measurements and scale counts for the holotype and paratypes are provided in Table 2. Body scales are similar to those of other geckos from Puerto Rico (e.g., members of the *S. macrolepis* complex; Daza et al., 2019), in having acute, flattened, keeled, and imbricate scales in the dorsum and limbs; rounded, flattened, keeled, and imbricated scales in the abdomen; escutcheon scales that extend into the ventral surface of the thighs, almost reaching the back of the knee (popliteal region); and subcaudal scales that are also rounded like the abdomen scales, but these are 2 or 3 times larger and unkeeled. Cephalic scales include: 1 subdivided rostral, 3 internasals, 3 supralabials, 3 infralabials, 1 mental, and 2 postmentals. The dorsal cephalic scales (Fig. 2) include juxtaposed hexagonal or rhomboid keeled canthals, which transition into juxtaposed, oval, keeled frontals and supraorbitals. The parietals are juxtaposed, rhomboid, and keeled. The transition to neck scales is gradual, and in the neck area, the scales duplicate in size and become more imbricated and pointed. In the ventral side (Fig. 2), there is a large mental scale, followed by 2 hexagonal postmentals. Gular scales are mostly unkeeled, but the scales adjacent to the infralabials are strongly keeled and look like elongated hexagons. In the gular area, there are scattered keeled scales, and a transition from hexagonal to rounded scales occurs. Scales become markedly keeled in the neck ventral region.

Color and pattern.—*The ground color of *S. verdeluzicola* is typically light brown with scattered light (yellowish or greenish cream) and dark (chestnut to dark brown) markings including lines, spots, and patches. *Sphaerodactylus verdeluzicola* displays a dark supraocular wedge, and a characteristic light-colored cephalic figure which resembles a club shape. *Sphaerodactylus verdeluzicola* displays a dark pentagonal parietal patch with the point aiming towards the snout (Figs. 2, 3), with the peak of the pentagon formed by a single scale. The maximum width of the parietal patch is about one-third the overall head breadth. There are two symmetrical dark nuchal patches, bounded caudally and medially by light lines, together defining an "L" or "C" shape. The nuchal patches are not continuous with the scapular patch.

Two narrow dark lines extend from the flanks of the parietal patch towards the interorbital area in a "V" shape, bounding a ground color cephalic figure, and ending abruptly at the rostral margin of the eye without contacting each other. Anteriorly, the two lines become continuous with dark gray coloration around the eyes. A lighter (cream) postocular stripe is present lateral to these two dark stripes and extends from the eye to the margin of the parietal patch. The postocular stripe is about three scales thick and is bounded inferiorly by a narrow dark stripe that is one or two scales thick. A dark brown canthal line is also present.

A dark scapular patch is present with two small white ocelli. The shape of the scapular patch resembles a bowtie, with two dark lateral rhombuses connected by a middle transverse line. There is a matching dark brown stripe on the lateral side of each ocellus, about one or two scales wide and about as long as the medial line. There are two lighter lines in

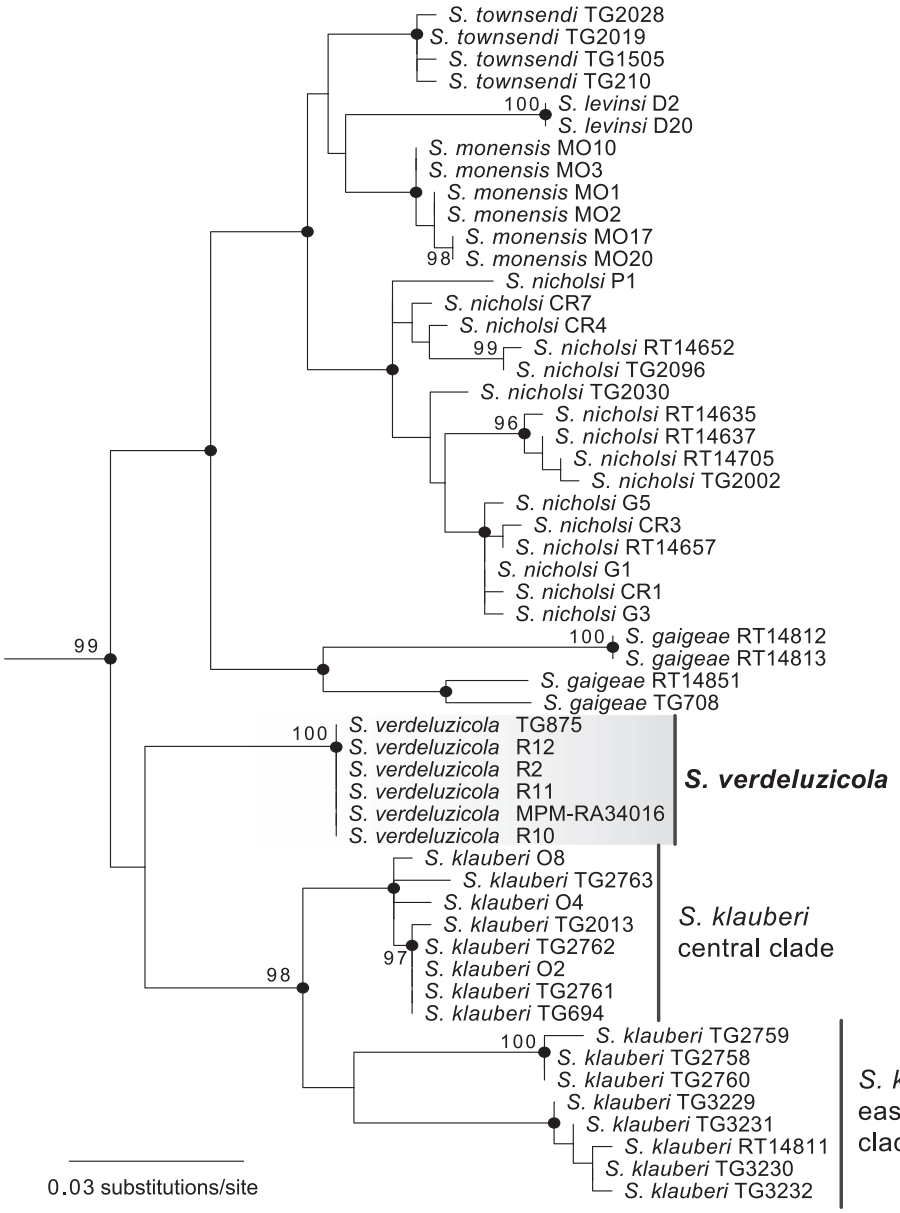

Fig. 4. Phylogenetic relationships among a subset of Puerto Rican species of *Sphaerodactylus*. Maximum likelihood phylogeny constructed using mitochondrial *16S* rRNA gene sequences with UFBoot values ≥95 adjacent to respective branches. Bayesian posterior probabilities ≥0.95 are indicated by black circles at nodes. Sequences of *Sphaerodactylus verdeluzicola* are highlighted by the gray box. Outgroup taxa (Table 1) pruned for clarity. See Data Accessibility for tree file.

bone brown color, one or two scales thick, lateral to the dark lines. An additional dark line in dark brown, one to two scales thick, is also present lateral to the light lines. These light-dark lines extend just caudal to the patch along the sides of the body.

The dorsal tail is the same color as the dorsum of the body. Markings in the pygal region include a dark brown chevron with the tip of the "V" pointing caudally, bound by cream or white posterior margins (Fig. 2). Laterally, there is a light-colored stripe, one to two scales thick, with dark brown lines (one to two scales thick) running parallel above and below. The ventrum is light colored, and a few dark scales can be found scattered on the ventral surface (Fig. 2). The dorsal ground color extends laterally onto the sides of the ventrum. There is a lighter patch of color extending from the lower ventrum to the thighs and the escutcheon region. The light stripe and vent are light yellowish cream. The tail is light cream-colored ventrally, with more dark spotting than the ventrum proper.

Color differences between live and alcohol-preserved specimens.—Dorsal color in the live animals is typically lighter and brighter than in alcohol-preserved specimens, which appear darker overall. The light ventral color may vary from cream to straw-colored in alcohol-preserved specimens. Red coloration on the tail, when present, also fades in the alcohol-preserved specimens. Nonetheless, the pattern in alcohol-preserved specimens remains clearly distinguishable.

Morphological variation.—Using collected specimens, we determined that adult SVL ranged from 19.49 mm to 25.48 mm ($\bar{x}$ = 21.293±1.78 mm; n = 24). Live adults weighed between 0.20 g and 0.50 g ($\bar{x}$ = 0.31±0.07 g; n = 32). Three gravid females weighed between 0.35–0.50 g. Male–female differences in size are also shown in Figure 5, using only vouchered specimens. *Sphaerodactylus verdeluzicola* in Rincón (Fig. 1) has smooth (unkeeled), slightly round pectoral scales that are juxtaposed rather than imbricated, while all specimens from Bosque Estatal de Río Abajo have slightly

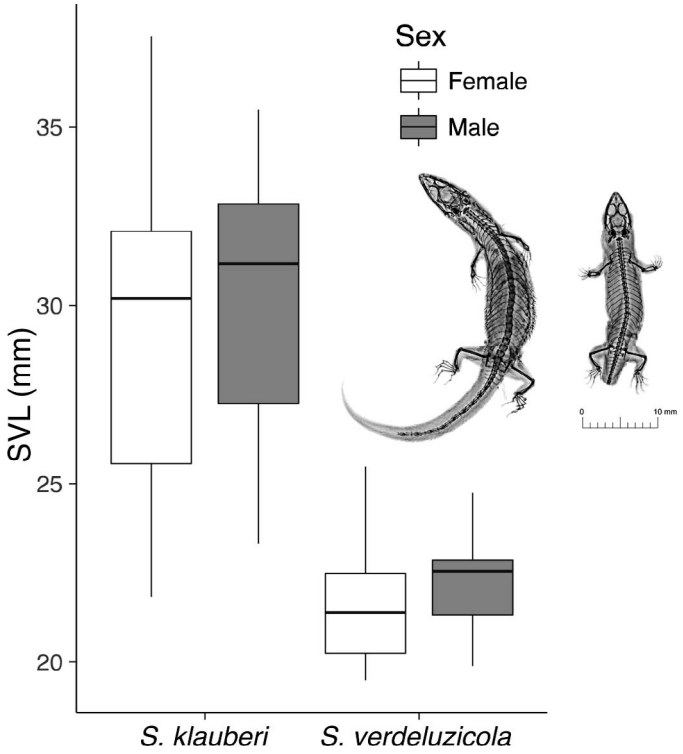

Fig. 5. Dot-box plot of SVL range between males and females of *S. verdeluzicola* and *S. klauberi*. Digital X-rays of the holotype of *Sphaerodactylus klauberi* (USNM 120719, left) and one specimen of *S. verdeluzicola* (MPM-RA34016, right) were added to the figure as a visual reference of the size difference between the two species.

overlapping, rhomboid pectoral scales with faint, partial keels (Fig. 6).

Although the majority of specimens have a light brown ground color with variable spotting patterns, some specimens display a darker or more uniform brown coloration. There is no sexual dichromatism in *S. verdeluzicola* (Fig. 5). Juveniles generally have more distinct markings with brighter light colors and darker dark colors than the adults, but otherwise do not differ from the adults in the pattern of coloration.

Iris color varies from amber to red (Fig. 3). The dorsal head pattern can be variable (Figs. 2, 3). The dark gray coloration around the eyes is not present in all individuals, and as a result the dark stripes on the face are not always continuous with the dark eye coloration. When present, the dark eye coloration may also have some green. The pentagonal parietal patch varies in size (8 to 10 scales long). Some parietal spots are more triangular or heart-shaped than pentagonal but are always dark, with the tip pointing rostrally. Although the dark stripes lateral to the parietal patch extend caudally and laterally in some specimens, in others the two stripes never extend caudal to the parietal spot. The light stripe lateral to the parietal patch is always present but may be from one scale up to six scales wide and may vary in color. The size and density of the nuchal patches vary from a few dark scales on either side to two large patches covering most of the nuchal area, which sometimes join to form one continuous patch. Occasionally the nuchal patches are continuous with the parietal patch.

The size, shape, and color intensity of the scapular patch varies. In some specimens, the patch is more square-shaped and solidly filled with the dark brown color, but in other specimens the patch is less distinctly separated from the ground color. In some cases, it lacks the transverse connecting line altogether or displays only one or two dark lines medial to each ocellus (Figs. 2, 3). Some specimens display a medial longitudinal line at the center of the patch, and sometimes this medial line joins the lateral stripes caudal to the ocelli. The medial line ranges from one or two scales longitudinally to an extended stripe up to 12 scales long. Ocelli in the scapular patch typically comprise one scale but can be as large as three or four scales forming a triangle or diamond pattern, and they range in color from white to tan. The light dorsolateral lines extend significantly beyond the caudal border of the scapular patch, but they are sometimes surrounded by an additional dark stripe.

Markings on the dorsum of the tail are variable, but in addition to the typical dark-light chevrons there are sometimes additional spots or blotches present on the tail, following the same dark-light pattern. The lateral stripes on the tail are always present but vary in length. Ventrally, some males can also have stippled oblique lateromedial lines on the throat. A dark stripe is sometimes present anterior to the vent and some individuals have an abrupt change in coloration at the escutcheon area. Some individuals display yellow to red coloration on the ventral side of the tail. The number of lamellae in the foot IV toe differs between populations of *S. verdeluzicola*. The specimens of *S. verdeluzicola* from Rincón fluctuate between 6 and 9 (median = 8, n = 8) lamellae, while in the Bosque Estatal de Río Abajo population the number ranges between 9 and 12 (median = 10, n = 17) lamellae. The Bosque Estatal de Río Abajo population overlaps in this trait with populations of *S. klauberi* from El Yunque, which have between 11 and 13 (median = 12, n = 7) lamellae.

Geographic distribution.—*Sphaerodactylus verdeluzicola* is found in low elevation areas (below 500 m.a.s.l.) in the northwest limestone region of Puerto Rico, encountered near the localities of Rincón, Isabela, Quebradillas, Bosque Estatal de Río Abajo (Arecibo and Utuado), Camuy, and Florida (Fig. 1).

Etymology.—Specific epithet *verdeluzicola* is derived from the Spanish phrase "verde luz" with the suffix *-cola* to indicate that it is a *Sphaerodactylus* gecko dwelling in the place where the green light shines. The name is a tribute to the song *Verde Luz*, considered by some the second national anthem of Puerto Rico, by singer-songwriter Antonio Cabán Vale "El Topo." The song expresses a sentiment of longing for the homeland, while in the diaspora, and praises the natural wonders of Puerto Rico, such as the exquisite beaches, its karst terrain, and the emerald light emanating from the mountains and the sea—scenery that correlates with this gecko's habitat. Furthermore, Antonio Cabán Vale grew up in the town of Moca in northwestern Puerto Rico, which is within the current distribution of *S. verdeluzicola*.

Phylogenetic analysis.—*Sphaerodactylus verdeluzicola* from Rincón and Bosque Estatal de Río Abajo share *16S* haplotypes. *Sphaerodactylus verdeluzicola* forms a well-supported clade to the exclusion of the samples of *S. klauberi* from central and eastern Puerto Rico, which includes the type locality of *S. klauberi*, El Yunque (Figs. 1, 4). Importantly, the

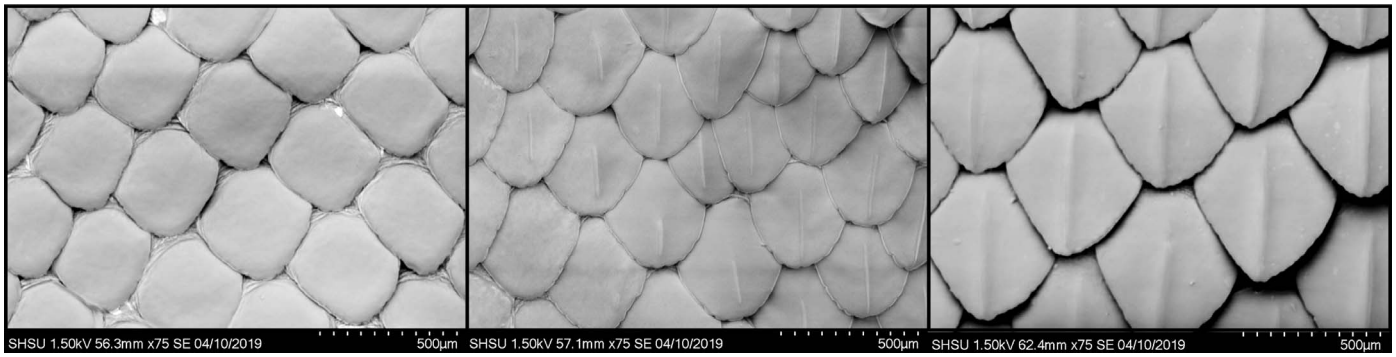

Fig. 6. Pectoral scales of *Sphaerodactylus verdeluzicola* and *S. klauberi*. Smooth scales in a specimen from Rincón (TG 2645, left), faintly keeled scales from a Bosque Estatal de Río Abajo individual (JDD 048, middle), and proportionally larger and strongly keeled scales in *S. klauberi* (TG 2758) from El Yunque (right).

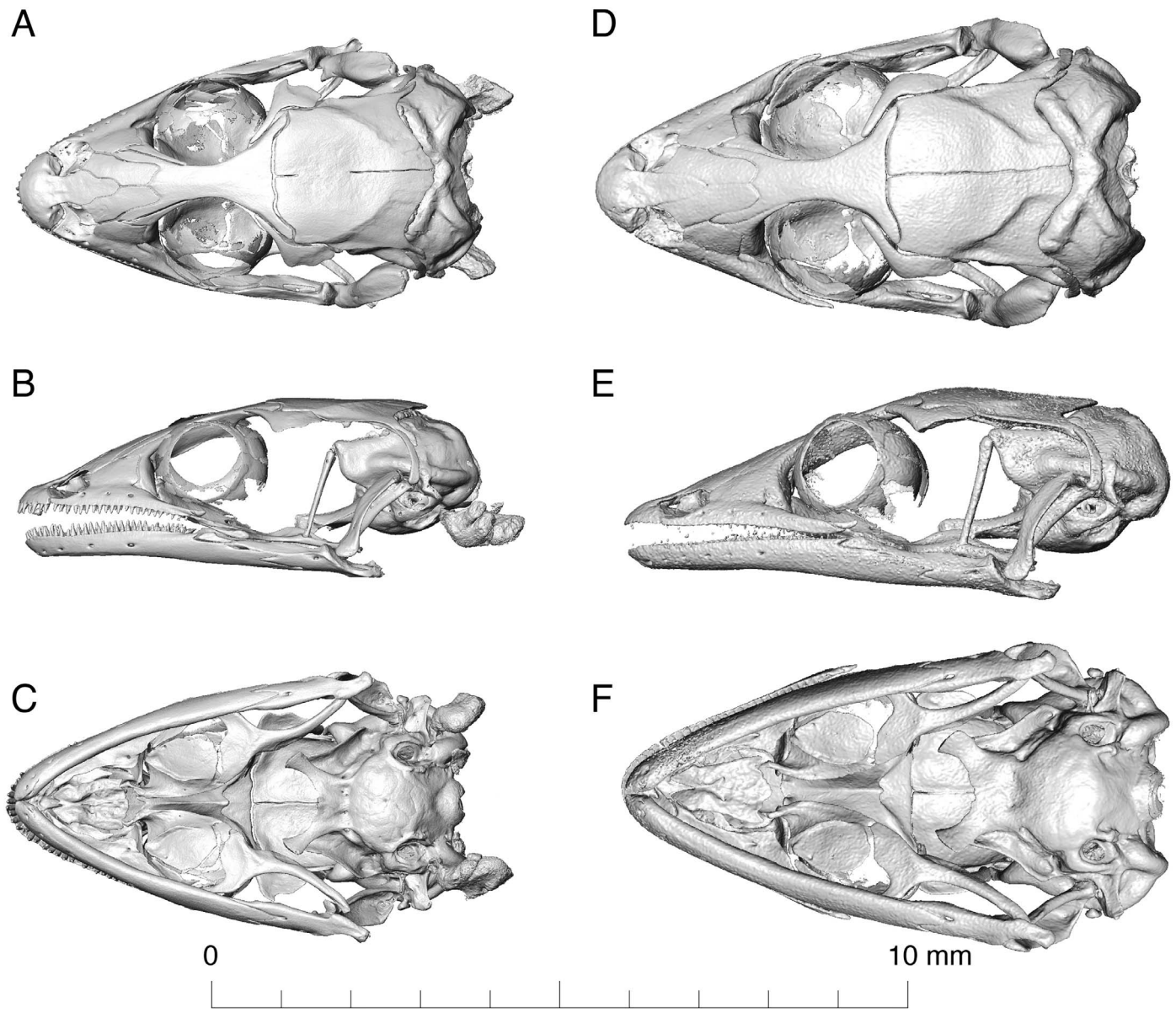

Fig. 7. Skull high resolution computed tomography images of *Sphaerodactylus verdeluzicola* and *S. klauberi*. (A–C) *Sphaerodactylus verdeluzicola* from Rincón (MPM-RA34016, holotype); (D–F) *Sphaerodactylus klauberi* from El Yunque (JDD 449). Notice the poorly ossified region along the tooth-bearing bones in *S. klauberi*; this phenomenon was present in both CT scanned specimens from El Yunque.

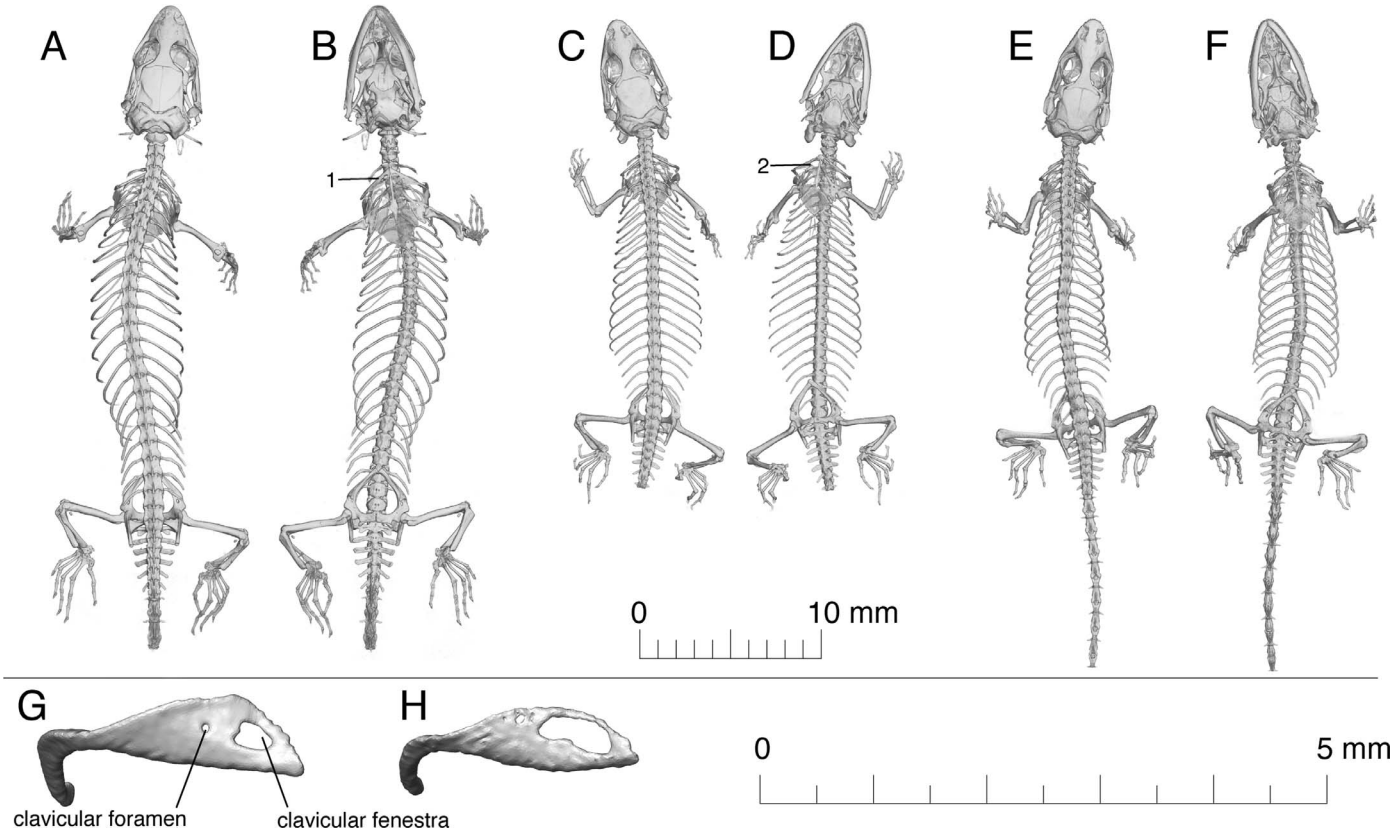

Fig. 8. Full body high resolution computed tomography of *Sphaerodactylus klauberi* and *S. verdeluzicola*. (A–B) *Sphaerodactylus klauberi* from the type locality—El Yunque (JDD 449); (C–D) *S. verdeluzicola* from Rincón (MPM-RA34016); (E–F) *S. verdeluzicola* from Bosque Estatal de Río Abajo (MPM-RA34019, male). (1) Indicates a clavicular fenestra, completely enclosed on bone; (2) indicates a nearly emarginate clavicular fenestra. Right clavicle of (G) *S. klauberi* (JDD 449) and (H) *S. verdeluzicola* (MPM-RA34019) showing the difference in size and position of the clavicular fenestra and the clavicular foramen.

inclusion of sequences of *S. klauberi* from near the type locality here confirms the uniqueness of *S. verdeluzicola* in relation to *S. klauberi sensu stricto*. Topologies were similar between the maximum likelihood and Bayesian trees at well-supported nodes (Fig. 4). Genetic distances between *S. verdeluzicola* and the central and eastern *S. klauberi* clades varied by 5.1% and 5.6%, respectively (Table 3).

Habitat and population density.—*Sphaerodactylus verdeluzicola* was found on the moist karst (limestone) hills of the municipality of Rincón and on the Bosque Estatal de Río Abajo, located between the municipalities of Arecibo and Utuado in Puerto Rico. Archival specimens labeled as *S. klauberi*, but matching the characteristics of *S. verdeluzicola*, were collected in the municipalities of Isabela, Quebradillas, Camuy, and Florida (Fig. 1). The species occurs in the Subtropical Moist Forest Ecological Life Zone (Ewel and Whitmore, 1973). Like most members of the genus *Sphaerodactylus*, *S. verdeluzicola* inhabits moist, dense leaf litter. The Rincón population was mainly found in leaf litter composed of María (*Calophyllum antillanum*), Almendro (*Terminalia catappa*), and Coconut Palm (*Cocos nucifera*, including decomposing fruit; Table S1; see Data Accessibility). Some other vegetation found in areas occupied by the geckos included (in order of frequency): Seagrape (*Coccoloba uvifera*), Almácigo (Gumbo limbo; *Bursera simaruba*), Emajaguilla (Portia tree; *Thespecia populnea*), Tintillo (White Indigo Berry; *Randia aculeata*), and Mahogany (*Swietenia mahagoni*; see Table S1 for more details; see Data Accessibility). The Río Abajo population was found deep within the dense forest, where vegetation is composed of species such as Algarrobo (Carob; *Ceratonia siliqua*), Almácigo (Gumbo limbo; *Bursera simaruba*), Palma de abanico (*Coccothrinax barbadensis*), Palma de escoba (Brittle thatch palm; *Leucothrinax morrisii*), Higuerillo (*Piper blattarum*), Ortiga (Stinging nettle; *Urera baccifera*), Corcho (*Guapira obtusata*), and Ceiba (Silk cotton tree; *Ceiba pentandra*; Little et al., 1974).

Observations of the Rincón population provide a preliminary look into the natural history of *S. verdeluzicola*. Over 195 m^2 were surveyed in three areas, north of Domes beach, east of Domes beach, and Punta Gorda. Population densities were estimated to be 4,167; 4,582; and 3,235 individuals/ha ($\sim$1 individual per 2 m^2), respectively. If the total surveyed area is pooled, the Rincón population density is an estimated 3,983 individuals/ha. *Sphaerodactylus verdeluzicola* was most commonly found in the following conditions: leaf litter humidity that ranged from 82–86%, soil humidity that ranged from 74–79%, soil temperature that ranged from 26–27°C (79.5–81.3°F), and at elevations that ranged from 5–47 m (Tables 4, S1; see Data Accessibility). Multiple ecological factors were analyzed at each survey plot (air humidity, air temperature, leaf litter temperature, leaf litter humidity, soil temperature, soil humidity, and elevation). Only soil humidity showed a slight significant difference (single factor ANOVA, $P = 0.05$) between occupied and empty sites. Individuals were found in plots with soil humidity ranging

Table 4. Environmental factors of surveyed sites where *Sphaerodactylus verdeluzicola* was present. A total of 39 plots were surveyed in the Municipality of Rincón, within a span of 4 days in early June 2019.

Factor		Mean ± SD	95% CI	Maximum	Minimum
Humidity (%)	Air at 1 m	79.23±6.64	(76.85, 81.60)	90.80	67.20
	Leaf litter	84.23±5.22	(82.36, 86.10)	92.60	74.70
	Soil	76.47±5.87	(74.37, 78.57)	87.00	64.00
Temperature (°C)	Air at 1 m	29.39±1.90	(28.36, 30.42)	32.06	24.17
	Leaf litter	29.73±1.98	(28.67, 30.80)	32.78	24.39
	Soil	26.91±1.45	(26.12, 27.69)	28.89	23.89
Elevation (m)		22.07±11.77	(17.85, 26.28)	47.00	5.00

from 74–79% (Tables 4, S1; see Data Accessibility). Most empty plots (5 out of 7) had a soil humidity higher than 85%.

DISCUSSION

As a first step towards the taxonomic resolution of groups within *S. klauberi* complex, we formally describe the lowland northwestern population, a forest-dwelling ecomorph, as a separate species, concurrently restricting *S. klauberi* to populations found in high elevations of El Yunque Forest, the Sierra de Cayey, and the Cordillera Central (Fig. 1). *Sphaerodactylus verdeluzicola* corresponds to Cluster I in Thomas and Schwartz (1966), *Sphaerodactylus* spp. [sic] in Díaz-Lameiro et al. (2013), and *S. klauberi* Northwest clade in Daza et al. (2019), but we here provide evidence that it is distinct from *S. klauberi* based on clear differences in size, scale morphology, coloration, skull morphology, and genetic distance.

The taxonomy and systematics of PRA *Sphaerodactylus* have been reviewed extensively (Günther, 1859; Stejneger, 1902; Grant, 1931, 1932b, 1932c; Thomas and Schwartz, 1966; Hass, 1991, 1996; Powell and Henderson, 2001; Padilla, 2008; Díaz-Lameiro et al., 2013; Daza et al., 2019; Pinto et al., 2019). Despite the attention, taxonomic classifications have remained relatively stable for many years. The latest taxonomic changes were the elevation of former subspecies of the *S. macrolepis* complex to species level, a reorganization that included: the elevation of *S. m. parvus* to species level, *S. parvus* (King, 1960, 1962; Powell and Henderson, 2001); the redefinition of *S. macrolepis* to the populations with a distribution range spanning from Eastern Culebra to the U.S. and British Virgin Islands (Daza et al., 2019); the elevation of *S. m. inigoi* to species level, *S. inigoi*, from Vieques Island and western Culebra Island (Daza et al., 2019); and the re-elevation of *S. grandisquamis*, narrowing this species to Puerto Rico, a satellite island (Isla Piñero), and two keys (Santiago and Batata; Daza et al., 2019). Indeed, *S. grandisquamis* was first proposed 116 years ago by Stejneger (Stejneger, 1902) and later reconsidered by Grant (1932c). Aside from the re-evaluation of *S. macrolepis* complex, no new endemic species of *Sphaerodactylus* has been described for the island of Puerto Rico in the last 88 years (Grant, 1932a). The relative taxonomic stability of *Sphaerodactylus* in Puerto Rico can be attributed to their conserved morphology and the limited availability of molecular data for the vast number of populations across the island. The discovery of *S. verdeluzicola* highlights the importance of ongoing biodiversity surveys and integrative taxonomy even in well-studied regions like Puerto Rico and in well-studied taxa such as reptiles. Accurate assessments of taxonomy and species diversity are necessary for establishing adequate conservation and management plans and preventing further loss of biodiversity.

The *16S* phylogeny (Fig. 4) was largely concordant with previously published mitochondrial gene trees at well-supported nodes (Díaz-Lameiro et al., 2013; Daza et al., 2019). Further, we have identified that *S. klauberi* from near the type locality form a well-supported mtDNA clade with *S. klauberi* from eastern and central Puerto Rico. Thus, we can rely on more extensive, previously published phylogenetic analyses to enhance our interpretation of these data. Indeed, Daza et al. (2019: fig. 4) identified a well-supported mtDNA clade (*S. verdeluzicola*) as sister to remaining *S. klauberi*. Corroborating the phylogenetic results, *16S* genetic distances between *S. verdeluzicola* and *S. klauberi* were between 5.1% and 5.6% (Table 3). This is comparable with the uncorrected p-distances between valid sister species of gecko for this locus, which range from 2% to >15% (Bauer and Lamb, 2002; Gamble et al., 2012; Metallinou et al., 2012; Daza et al., 2019; Pinto et al., 2019). In fact, this is greater than the 3% uncorrected sequence divergence in *16S* rRNA gene which has been used as a tentative cutoff for identifying cryptic species of amphibian and reptiles (Vieites et al., 2009). Genetic distances between the eastern and central clades of *S. klauberi sensu stricto* (3.1%) were also larger than distances among some recognized species pairs (Table 3), suggesting additional taxonomic work may be necessary in this species group.

We observed no variation among the *16S* rRNA gene haplotypes of *S. verdeluzicola*, including additional samples not used here (Díaz-Lameiro et al., 2013; Daza et al., 2019). However, the more variable mitochondrial locus, *ND2*, does show variation both within and between populations of *S. verdeluzicola* (Daza et al., 2019). The low genetic diversity reported here is likely an artifact of the slow evolutionary rate of *16S* rRNA gene relative to other mitochondrial loci (Mueller, 2006; Duchêne et al., 2011). Further sampling of populations of *S. verdeluzicola* with informative molecular markers are needed to fully characterize the genetic diversity within this species.

A pooled preliminary population density of 3,983 individuals/ha was estimated for the Rincón locality. An estimate higher than extremely low density species such as *S. sputator* (159, 195, and 72 individuals/ha; Hensley et al., 2004), *S. kirbyi* (196 individuals/ha; Bentz et al., 2011), *S. sabanus* (1,427, 1,757, and 727 individuals/ha; Hensley et al., 2004), and *S. fantasticus* on Dominica (1,210 individuals/ha; Turk et al., 2010). Yet, it was smaller than what has been reported for *S. vincenti vincenti* (5,625 individuals/ha; Steinberg et al., 2007), *S. physacinus* (7,900 individuals/ha; Breuil, 2002), *S. v. ronaldi* (8,220 individuals/ha; Leclair and Leclair, 2011), *S.*

fantasticus on Grand Terre (10,000 individuals/ha; Breuil, 2002), and *S. klauberi* (10,000 individuals/ha; Thomas and Kessler, 1996), and exceptionally small when compared to extremely dense species such as *S. parvus* (52,000 individuals/ha; Powell et al., 2001) and *S. macrolepis* (67,600 individuals/ha; Rodda et al., 2001).

Although population density for *S. verdeluzicola* in Rincón seems relatively sparse when compared to many other *Sphaerodactylus*, over the ten years of field visits the populations appear constant at both localities (Rincón and Bosque Estatal de Río Abajo). As data are limited to just a few geographically proximate populations/metapopulations, further surveys on population structure must be undertaken before species status can be addressed. Future work should focus on assessing population density in other localities to confirm the species distribution and status. Understanding population dynamics, density, and diversity of *S. verdeluzicola* will be instrumental in making future management and/or conservation decisions regarding the new species. Preliminary field data also suggested that soil humidity could be a delimiting factor for the species, although a more extensive survey, which includes the Río Abajo population, must be completed. Here we provide baseline information on the new species, *S. verdeluzicola*, as an introduction to scientific literature. This information is critical to further research in order to fully understand the natural history, evolution, ecology, and status of the new species.

MATERIAL EXAMINED

Institutional abbreviations follow Sabaj (2020). MPM, Milwaukee Public Museum.

Sphaerodactylus klauberi: Adjuntas: 18, SHSUHerp 000855–000866, 000871–000872, 000919, USNM 326955, 326958–326959; Canóvanas, El Yunque: 11, USNM 120719 (holotype), 326949–326952, 326962, SHSUHerp 000898–000900, 000902–000903; Cayey: 3, SHSUHerp 000916–000918; Fajardo, El Yunque: 1, SHSUHerp 000901; Jayuya, Toro Negro: 6, SHSUHerp 000851–000853, 000867, 000905–000906; Maricao: 4, USNM 292265–292266, 326956–326957; Orocovis: 8, SHSUHerp 000873–000879, 000907; Villalba: 3, SHSUHerp 000869, 000896–000897.

Sphaerodactylus verdeluzicola: Arecibo: 19 (2 paratypes), MPM-RA34018, 34019, SHSUHerp 000880–000895, 000904; Florida: 2, USNM 326953–326954; Rincón: 22, AMDLR 1901–1910, MPM-RA34016, 34017, SHSUHerp 000868, 000909–000912, 000920–000924.

DATA ACCESSIBILITY

Supplemental material is available at https://www.ichthyologyandherpetology.org/h2020123. Unless an alternative copyright or statement noting that a figure is reprinted from a previous source is noted in a figure caption, the published images and illustrations in this article are licensed by the American Society of Ichthyologists and Herpetologists for use if the use includes a citation to the original source (American Society of Ichthyologists and Herpetologists, the DOI of the *Ichthyology & Herpetology* article, and any individual image credits listed in the figure caption) in accordance with the Creative Commons Attribution CC BY License. ZooBank publication urn:lsid:zoobank.org:pub:F0FF0727-7051-4E8D-95A9-EFA3E32DCDC4.

ACKNOWLEDGMENTS

We would like to thank R. Bell, K. de Queiroz, K. Tighe, A. Wynn, and S. Gotte for facilitating access to the Smithsonian National Museum of Natural History Amphibian and Reptiles Collection and X-ray facilities; J. Colby and J. Zaspel for facilitating the accession of specimens to the Milwaukee Public Museum's herpetology collections; J. Ackerman for access to the Museo de Zoología de la Universidad de Puerto Rico, Recinto Río Piedras; J. Maisano and M. Colbert at the University of Texas High-Resolution X-Ray CT Facility for fast acquisition of HRCT data. We also thank C. Restrepo for supplying a topographic map of Puerto Rico, R. P. Balaraman from Sam Houston State University for scanning electron microscope images of pectoral scales. We also thank the Departamento de Recursos Naturales y Ambientales de Puerto Rico (DRNA) for collecting permits for scientific purposes (2019-IC-046, 2018-IC-032, 2016-IC-091, 2014-IC-042, and 2013-IC-006). Field study carried out in compliance with Towson University IACUC FIELD STUDY #1905000345 and Marquette University IACUC AR288. J.D.D. received funding from National Science Foundation (NSF) DEB 1657662 and the Biological Sciences Program at Sam Houston State University. T.G. received funding from National Science Foundation (NSF) DEB 1657648 and the Biological Sciences Program at Marquette University. A.M.D.L. received funding from the Biological Sciences Department at Towson University. Field trips were sponsored by the Biological Sciences Departments at Sam Houston State University, Towson University, Marquette University, University of Puerto Rico at Mayagüez, and the University of Texas at Arlington. The process from the species discovery to its description involved multiple field assistants, including Z. Brooks, R. Colón, F. A. Daza, R. Díaz, T. Eubank, M. "Toño" García, E. Glynne, W. Guiblet, S. B. Hedges, J. L. Herrera, N. Holovacs, R. Laver, D. Logue, E. D. Martínez, L. Martínez Díaz, M. T. Martínez, D. Martinó, S. Padrón, S. Ramirez, N. Rios, C. Rivera, V. Rodriguez, C. A. Rodríguez Gómez, C. T. Ruiz, E. Santiago, and D. Zarkower.

LITERATURE CITED

Allen, K. E., and R. Powell. 2014. Thermal biology and microhabitat use in Puerto Rican eyespot geckos (*Sphaerodactylus macrolepis macrolepis*). Herpetological Conservation and Biology 9:590–600.

Baeckens, S., S. P. Blomberg, and R. Shine. 2020. Inclusive science: ditch archaic terms. Nature 580:185.

Barbour, T. 1921. *Sphaerodactylus*. Memoirs of the Museum of Comparative Zoology at Harvard 47:217–278.

Bauer, A. M., and T. Lamb. 2002. Phylogenetic relationships among members of the *Pachydactylus capensis* group of southern African geckos. African Zoology 37:209–220.

Bentz, E. J., M. R. Rodríguez, R. R. John, R. W. Henderson, and R. Powell. 2011. Population densities, activity, microhabitats, and thermal biology of a unique crevice- and litter-dwelling assemblage of reptiles on Union Island, St. Vincent and the Grenadines. Herpetological Conservation and Biology 6:40–50.

Bouckaert, R., T. G. Vaughan, J. Barido-Sottani, S. Duchêne, M. Fourment, A. Gavryushkina, J. Heled, G.

Jones, D. Kühnert, N. De Maio, M. Matschiner, F. K. Mendes, N. F. Müller, H. A. Ogilvie . . . A. J. Drummond. 2019. BEAST 2.5: an advanced software platform for Bayesian evolutionary analysis. PLoS Computational Biology 15:e1006650.

Breuil, M. 2002. Histoire naturelle des amphibiens et reptiles terrestres de l'archipel guadeloupéen, Guadeloupe, Saint-Martin, Saint-Barthélémy. Collection Patrimoines Naturels 54:1–339.

Daza, J. D., V. Abdala, R. Thomas, and A. M. Bauer. 2008. Skull anatomy of the miniaturized gecko *Sphaerodactylus roosevelti* (Squamata: Gekkota). Journal of Morphology 269: 1340–1364.

Daza, J. D., B. J. Pinto, R. Thomas, A. Herrera-Martínez, D. P. Scantlebury, L. F. García, R. P. Balaraman, G. Perry, and T. Gamble. 2019. The sprightly little sphaerodactyl: systematics and biogeography of the Puerto Rican dwarf geckos *Sphaerodactylus* (Gekkota, Sphaerodactylidae). Zootaxa 4712:151–201.

Díaz-Lameiro, A. M., T. K. Oleksyk, F. J. Bird-Picó, and J. C. Martínez-Cruzado. 2013. Colonization of islands in the Mona Passage by endemic dwarf geckoes (genus *Sphaerodactylus*) reconstructed with mitochondrial phylogeny. Ecology and Evolution 3:4488–4500.

Duchêne, S., F. I. Archer, J. Vilstrup, S. Caballero, and P. A. Morin. 2011. Mitogenome phylogenetics: the impact of using single regions and partitioning schemes on topology, substitution rate and divergence time estimation. PLoS ONE 6:e27138.

Edgar, R. C. 2004. MUSCLE: multiple sequence alignment with high accuracy and high throughput. Nucleic Acids Research 32:1792–1797.

Ewel, J. J., and J. L. Whitmore. 1973. The Ecological Life Zones of Puerto Rico and the U.S. Virgin Islands. USDA Forest Service, Institute of Tropical Forestry, Research Paper ITF-018.

Gamble, T. 2014. Collecting and Preserving Genetic Material for Herpetological Research. Society for the Study of Amphibians and Reptiles, Salt Lake City, Utah.

Gamble, T., G. R. Colli, M. T. Rodrigues, F. P. Werneck, and A. M. Simons. 2012. Phylogeny and cryptic diversity in geckos (*Phyllopezus*; Phyllodactylidae; Gekkota) from South America's open biomes. Molecular Phylogenetics and Evolution 62:943–953.

Gamble, T., A. M. Simons, G. R. Colli, and L. J. Vitt. 2008. Tertiary climate change and the diversification of the Amazonian gecko genus *Gonatodes* (Sphaerodactylidae, Squamata). Molecular Phylogenetics and Evolution 46: 269–277.

GBIF Secretariat. 2020. GBIF Backbone Taxonomy. https://www.gbif.org/species/2445297 (accessed 5 May 2020).

Grant, C. 1931. The sphaerodactyls of Porto Rico, Culebra and Mona Islands. Journal of Agriculture University of Puerto Rico 15:199–213.

Grant, C. 1932a. A new sphaerodactyl from Porto Rico. The Journal of Agriculture of the University of Puerto Rico 16: 31.

Grant, C. 1932b. Chart for determining the sphaerodactyls of the Porto Rico region. The Journal of Agriculture of the University of Puerto Rico 16:33–35.

Grant, C. 1932c. *Sphaerodactylus grandisquamis*, a valid species. The Journal of Agriculture of the University of Puerto Rico 16:43–45.

Griffing, A. H., J. D. Daza, J. C. DeBoer, and A. M. Bauer. 2018. Developmental osteology of the parafrontal bones of the Sphaerodactylidae. The Anatomical Record 301:581–606.

Günther, A. 1859. On the reptiles from St. Croix, West Indies, collected by Messrs. A. and E. Newton. The Annals and Magazine of Natural History 3:209–217.

Hass, C. A. 1991. Evolution and biogeography of West Indian *Sphaerodactylus* (Sauria: Gekkonidae): a molecular approach. Journal of Zoology 225:525–561.

Hass, C. A. 1996. Relationships among West Indian geckos of the genus *Sphaerodactylus*: a preliminary analysis of mitochondrial 16S ribosomal RNA sequences, p. 175–194. *In*: Contributions to West Indian Herpetology: A Tribute to Albert Schwartz. R. Powell and R. W. Henderson (eds.). Society for the Study of Amphibians and Reptiles, Ithaca, New York.

Hedges, S. B., and R. Thomas. 2001. At the lower size limit in amniote vertebrates: a new diminutive lizard from the West Indies. Caribbean Journal of Science 37:168–173.

Henderson, R. W., and R. Powell. 2009. Natural History of West Indian Reptiles and Amphibians. University Press of Florida, Gainesville, Florida.

Hensley, R. L., S. M. Wissmann, R. Powell, and J. S. Parmerlee. 2004. Habitat preferences and abundance of dwarf geckos (*Sphaerodactylus*) on St. Eustatius, Netherlands Antilles. Caribbean Journal of Science 40:427–429.

Hoang, D. T., O. Chernomor, A. Von Haeseler, B. Q. Minh, and L. S. Vinh. 2018. UFBoot2: improving the ultrafast bootstrap approximation. Molecular Biology and Evolution 35:518–522.

Kalyaanamoorthy, S., B. Q. Minh, T. K. Wong, A. von Haeseler, and L. S. Jermiin. 2017. ModelFinder: fast model selection for accurate phylogenetic estimates. Nature Methods 14:587–589.

Kearse, M., R. Moir, A. Wilson, S. Stones-Havas, M. Cheung, S. Sturrock, S. Buxton, A. Cooper, S. Markowitz, C. Duran, T. Thierer, B. Ashton, P. Meintjes, and A. Drummond. 2012. Geneious basic: an integrated and extendable desktop software platform for the organization and analysis of sequence data. Bioinformatics 28:1647–1649.

King, W. 1960. The status of *Sphaerodactylus pictus*, with comments on the distribution of *S. sputator* and *S. sabanus*. Breviora 132:1–5.

King, W. 1962. Systematics of Lesser Antillean lizards of the genus *Sphaerodactylus*. Bulletin of the Florida State Museum 7:1–52.

Kumar, S., G. Stecher, and K. Tamura. 2016. MEGA7: molecular evolutionary genetics analysis version 7.0 for bigger datasets. Molecular Biology and Evolution 33:1870–1874.

Leclair, R., Jr., and M. H. Leclair. 2011. Life-history traits in a population of the dwarf gecko, *Sphaerodactylus vincenti ronaldi*, from a xerophytic habitat in Martinique, West Indies. Copeia 2011:566–576.

Little, E. L., R. O. Woodbury, and F. H. Wadsworth. 1974. Trees of Puerto Rico and the Virgin islands. U.S. Department of Agriculture, Forest Service.

López-Ortiz, R., and A. R. Lewis. 2002. Seasonal abundance of hatchlings and gravid females of *Sphaerodactylus nicholsi* in Cabo Rojo, Puerto Rico. Journal of Herpetology 36:276–280.

Lugo, A. E., L. Miranda Castro, A. Vale, T. M. López, E. Hernández Prieto, A. García Martinó, A. R. Puente Rolón, A. G. Tossas, D. A. McFarlane, T. Miller, A. Rodríguez, J. Lundberg, J. Thomlinson, J. Colón . . . E. Helmer. 2001. Puerto Rican Karst—A Vital Resource. United States Department of Agriculture Forest Service General Technical Report WO-65.

MacLean, W. P. 1982. Reptiles and Amphibians of the Virgin Islands. Macmillan Caribbean.

MacLean, W. P. 1985. Water-loss rates of *Sphaerodactylus parthenopion* (Reptilia: Gekkonidae), the smallest amniote vertebrate. Comparative Biochemistry and Physiology Part A: Physiology 82:759–761.

Metallinou, M., E. N. Arnold, P. A. Crochet, P. Geniez, J. C. Brito, P. Lymberakis, S. B. El Din, R. Sindaco, M. Robinson, and S. Carranza. 2012. Conquering the Sahara and Arabian deserts: systematics and biogeography of *Stenodactylus* geckos (Reptilia: Gekkonidae). BMC Evolutionary Biology 12:258.

Miller, M. A., W. Pfeiffer, and T. Schwartz. 2010. Creating the CIPRES Science Gateway for inference of large phylogenetic trees. Gateway Computing Environments Workshop (GCE) 2010:1–8.

Monroe, W. H. 1976. The karst landforms of Puerto Rico. U.S. Geological Survey Professional Paper 899.

Mueller, R. L. 2006. Evolutionary rates, divergence dates, and the performance of mitochondrial genes in Bayesian phylogenetic analysis. Systematic Biology 55:289–300.

Nei, M., and W. H. Li. 1979. Mathematical model for studying genetic variation in terms of restriction endonucleases. Proceedings of the National Academy of Sciences of the United States of America 76:5269–5273.

Nguyen, L. T., H. A. Schmidt, A. Von Haeseler, and B. Q. Minh. 2015. IQ-TREE: a fast and effective stochastic algorithm for estimating maximum-likelihood phylogenies. Molecular Biology and Evolution 32:268–274.

Padilla, L. F. 2008. Geographic variation in color pattern of the Gecko: *Sphaerodactylus macrolepis* (Sauria: Gekkonidae). Unpubl. Ph.D. diss., Universidad de Puerto Rico.

Pinto, B. J., J. Titus-McQuillan, J. D. Daza, and T. Gamble. 2019. Persistence of a geographically-stable hybrid zone in Puerto Rican dwarf geckos. Journal of Heredity 110:523–534.

Pisani, G. R. 1973. A guide to preservation techniques for amphibians and reptiles. Miscellaneous Publications, Herpetological Circular No.1, The Society for the Study of Amphibians and Reptiles, Lawrence, Kansas.

Powell, R., and R. W. Henderson. 2001. On the taxonomic status of some Lesser Antillean lizards. Caribbean Journal of Science 37:288–290.

Powell, R., R. Henderson, C. Lindsay, and S. Nava. 2001. Microhabitat, activity, and density of a dwarf gecko (*Sphaerodactylus parvus*) on Anguilla, West Indies. Amphibia-Reptilia 22:455–464.

Pregill, G. 1981. Late Pleistocene herpetofaunas from Puerto Rico. Miscellaneous Publications of the University of Kansas Museum of Natural History 71:1–72.

R Core Team. 2019. R: a language and environment for statistical computing. R Foundation for Statistical Computing, Vienna, Austria. https://www.R-project.org/

Rambaut, A., A. J. Drummond, D. Xie, G. Baele, and M. A. Suchard. 2018. Posterior summarization in Bayesian phylogenetics using Tracer 1.7. Systematic Biology 67: 901–904.

Rivero, J. A. 1998. Amphibians and Reptiles of Puerto Rico. La Editorial, Universidad de Puerto Rico.

Rivero, J. A. 2006. Guía Para la Identificación de Lagartos y Culebras de Puerto Rico. La Editorial, Universidad de Puerto Rico.

Rodda, G. H., G. A. Perry, R. J. Rondeau, and J. Lazell. 2001. The densest terrestrial vertebrate. Journal of Tropical Ecology 17:331–338.

Sabaj, M. H. 2020. Codes for natural history collections in ichthyology and herpetology. Copeia 108:593–669.

Schindelin, J., I. Arganda-Carreras, E. Frise, V. Kaynig, M. Longair, T. Pietzsch, S. Preibisch, C. Rueden, S. Saalfeld, B. Schmid, and J. Y. Tinevez. 2012. Fiji: an open-source platform for biological-image analysis. Nature Methods 9: 676–682.

Schwartz, A. 1973. *Sphaerodactylus*. Catalogue of American Amphibians and Reptiles (CAAR) 142.1–142.2.

Schwartz, A., and R. W. Henderson. 1991. Amphibians and Reptiles of the West Indies: Descriptions, Distributions, and Natural History. University Press of Florida, Gainesville, Florida.

Steinberg, D. S., S. D. Powell, R. Powell, J. S. Parmerlee, and R. W. Henderson. 2007. Population densities, water-loss rates, and diets of *Sphaerodactylus vincenti* on St. Vincent, West Indies. Journal of Herpetology 41:330–336.

Stejneger, L. 1902. Herpetology of Porto Rico. United States Natural Museum Annual Report.

Tavaré, S. 1986. Some probabilistic and statistical problems in the analysis of DNA sequences. Lectures on Mathematics in the Life Sciences 17:57–86.

Thomas, R. 1965. A new gecko from the Virgin Islands. Quarterly Journal of the Florida Academy of Sciences 28: 117–122.

Thomas, R. 1999. The Puerto Rico area, p. 169–179. *In*: Caribbean Amphibians and Reptiles. B. I. Crother (ed.). Academic Press, San Diego.

Thomas, R., S. B. Hedges, and O. H. Garrido. 1992. Two new species of *Sphaerodactylus* from eastern Cuba (Squamata: Gekkonidae). Herpetologica 48:358–367.

Thomas, R., and A. G. Kessler. 1996. Nonanoline reptiles, p. 347–362. *In*: The Food Web of a Tropical Rain Forest. D. P. Reagan and R. B. Waide (eds.). University of Chicago Press, Chicago.

Thomas, R., and A. Schwartz. 1966. *Sphaerodactylus* (Gekkonidae) in the greater Puerto Rico region. Bulletin of Florida State Museum 10:193–260.

Thomas, R., and A. Schwartz. 1975. A Check-list of West Indian Amphibians and Reptiles. Carnegie Museum of Natural History, Special Publication 1:1–216.

Turk, P. A., N. N. Wyszynski, R. Powell, and R. W. Henderson. 2010. Population densities and water-loss rates of *Gymnophthalmus pleii*, *Gymnophthalmus underwoodi* (Gymnophthalmidae), and *Sphaerodactylus fantasticus fuga* (Sphaerodactylidae) on Dominica, West Indies. Salamandra 46:125–130.

Vieites, D. R., K. C. Wollenberg, F. Andreone, J. Köhler, F. Glaw, and M. Vences. 2009. Vast underestimation of Madagascar's biodiversity evidenced by an integrative amphibian inventory. Proceedings of the National Academy of Sciences of the United States of America 106:8267–8272.

Wickham, H. 2016. ggplot2: Elegant Graphics for Data Analysis. Springer-Verlag, New York.